Published in final edited form as:
Cancer Cell. 2014 September 8; 26(3): 319–330. doi:10.1016/j.ccr.2014.07.014.

The somatic genomic landscape of chromophobe renal cell carcinoma

Caleb F. Davis[1,*], **Christopher Ricketts**[2,*], **Min Wang**[1,*], **Lixing Yang**[3,*], **Andrew D. Cherniack**[4], **Hui Shen**[5], **Christian Buhay**[1], **Hyojin Kang**[33], **Sang Cheol Kim**[6], **Catherine C. Fahey**[7], **Kathryn E. Hacker**[7], **Gyan Bhanot**[8,9], **Dmitry A. Gordenin**[10], **Andy Chu**[11], **Preethi H. Gunaratne**[1,12], **Michael Biehl**[13], **Sahil Seth**[14], **Benny A. Kaipparettu**[15,16], **Christopher A. Bristow**[14], **Lawrence A. Donehower**[1], **Eric M. Wallen**[17], **Angela B. Smith**[17], **Satish K. Tickoo**[18], **Pheroze Tamboli**[19], **Victor Reuter**[18], **Laura S. Schmidt**[2,20], **James J. Hsieh**[21,22], **Toni K. Choueiri**[23,24], **A. Ari Hakimi**[25], **The Cancer Genome Atlas Research Network**[**], **Lynda Chin**[4,14], **Matthew Meyerson**[4,23], **Raju Kucherlapati**[26,27], **Woong-Yang Park**[6,28], **A. Gordon Robertson**[11], **Peter W. Laird**[5], **Elizabeth P. Henske**[4,23,24], **David J. Kwiatkowski**[4,23,24], **Peter J. Park**[3,26], **Margaret Morgan**[1], **Brian Shuch**[28], **Donna Muzny**[1], **David A. Wheeler**[1], **W. Marston Linehan**[2], **Richard A. Gibbs**[1], **W. Kimryn Rathmell**[17,30,31,†], and **Chad J. Creighton**[1,15,32,†]

[1]Human Genome Sequencing Center, Baylor College of Medicine, Houston, TX 77030

[2]Urologic Oncology Branch, Center for Cancer Research, National Cancer Institute CRC Room 1W-5940 Bethesda, Maryland 20892

[3]Center for Biomedical Informatics, Harvard Medical School, Boston, MA 02115

[4]The Eli and Edythe L. Broad Institute of Massachusetts Institute of Technology and Harvard University Cambridge, Massachusetts 02142

Correspondence to: Chad J. Creighton (creighto@bcm.edu) and W. Kimryn Rathmell (rathmell@med.unc.edu).
*co-first authors
†co-senior authors
**Complete list of authors appears at the end of the manuscript.

Author Contributions: The Cancer Genome Atlas consortium contributed collectively to this study. Biospecimens were provided by the Tissue Source Sites and processed by the Biospecimen Core Resource. Data generation and analyses were performed by the Genome Sequencing Center, Genome Characterization Centers and Genome Data Analysis centers. All data were released through the Data Coordinating Center. Project activities were coordinated by the NCI and NHGRI Project Teams. Initial guidance in the project design was provided by the Disease Working Group. We also acknowledge the following TCGA investigators of the Analysis Working Group who contributed substantially to the analysis and writing of this manuscript: **Project leaders:** Chad J. Creighton, W. Kimryn Rathmell. **Data Coordinator:** Margaret Morgan. **Manuscript Coordinator:** Brian Shuch. **Analysis Coordinator:** Chad J. Creighton. **Writing Team:** Chad J. Creighton, Richard A. Gibbs, Elizabeth P. Henske, David J. Kwiatkowski, W. Marston Linehan, W. Kimryn Rathmell, Christopher Ricketts, Brian Shuch. **DNA Sequence Analysis:** Caleb F. Davis, Dmitry A. Gordenin, Hyojin Kang, Sang Cheol Kim, Peter J. Park, David A. Wheeler, Lixing Yang. **mRNA Analysis:** Gyan Bhanot, Michael Biehl, Catherine C. Fahey, Kathryn E. Hacker. **microRNA Analysis:** Andy Chu, Preethi H. Gunaratne, A. Gordon Robertson. **DNA Methylation Analysis:** Hui Shen, Peter W. Laird. **Copy Number Analysis:** Andrew D. Cherniack. **Mitochondrial Analysis:** Donna Muzny, Christopher A. Bristow, Christian Buhay, Benny A. Kaipparettu, Sahil Seth, Min Wang. **Pathway Analysis:** Lawrence A. Donehower, David J. Kwiatkowski, Christopher Ricketts. **Clinical Data:** Angela B. Smith, Eric M. Wallen. **Pathology and Clinical Expertise:** Toni K. Choueiri, A. Ari Hakimi, Elizabeth P. Henske, James J. Hsieh, W. Marston Linehan, W. Kimryn Rathmell, Victor Reuter, Laura S. Schmidt, Brian Shuch, Pheroze Tamboli, Satish K. Tickoo.

[5]USC Epigenome Center, University of Southern California, Los Angeles, CA 90033

[6]Samsung Genome Institute, Samsung Medical Center, Seoul, Korea

[7]Curriculum in Genetics and Molecular Biology, Lineberger Comprehensive Cancer Center, University of North Carolina, Chapel Hill, NC 27599

[8]Department of Molecular Biology and Biochemistry, Rutgers University, Busch Campus, Piscataway, NJ 08854

[9]Cancer Institute of New Jersey, 195 Little Albany Street, New Brunswick, NJ 08903

[10]National Institute of Environmental Health Sciences, 111 T.W. Alexander Drive, Research Triangle Park, NC 27709

[11]Canada's Michael Smith Genome Sciences Centre, BC Cancer Agency, Vancouver, BC V5Z 4S6

[12]Department of Biology & Biochemistry, University of Houston, 4800 Calhoun Road, Houston, TX 77204

[13]University of Groningen, Johann Bernoulli Institute for Mathematics and Computer Science, Intelligent Systems Group, P.O. Box 407, 9700 AK Groningen

[14]Institute for Applied Cancer Science, Department of Genomic Medicine, The University of Texas MD Anderson Cancer Center, Houston, TX 77030

[15]Dan L. Duncan Cancer Center, Baylor College of Medicine, Houston, TX 77030

[16]Department of Molecular and Human Genetics, Baylor College of Medicine, Houston, TX 77030

[17]Department of Urology, University of North Carolina, Chapel Hill, NC 27599

[18]Department of Pathology, Memorial Sloan-Kettering Cancer, 1275 York Avenue, New York, NY 10065

[19]Department of Pathology, The University of Texas, M.D. Anderson Cancer Center, 1515 Holcombe Boulevard, Houston TX 77030

[20]Leidos Biomedical Research, Inc., Basic Science Program, Frederick National Laboratory for Cancer Research, Frederick, MD 21702

[21]Department of Medicine, Weill-Cornell Medical College, New York, NY10021

[22]Human Oncology and Pathogenesis Program, Memorial Sloan-Kettering Cancer Center, New York, NY 10065

[23]Department of Medical Oncology, Dana-Farber Cancer Institute, 450 Brookline Ave, Boston, MA 02215

[24]Department of Medicine, Harvard Medical School, Boston, MA 02215

[25]Department of Surgery, Urology Service Memorial Sloan Kettering Cancer Center, New York, NY 10065

[26]Department of Genetics, Harvard Medical School, Boston, MA 02115

[27]Division of Genetics, Brigham and Women's Hospital, Boston, MA 02115

[28]Sungkyunkwan University School of Medicine, Seoul, Korea

[29]Department of Urology, Yale School of Medicine, New Haven, CT 06520

[30]Department of Genetics, University of North Carolina at Chapel Hill, Chapel Hill, NC 27599

[31]Department of Medicine, Division of Hematology and Oncology, University of North Carolina, Chapel Hill, NC 27599

[32]Department of Medicine, Baylor College of Medicine, Houston, TX 77030

[33]National Institute of Supercomputing and Networking, Korea Institute of Science and Technology Information, Daejeon, Korea

Summary

We describe the landscape of somatic genomic alterations of 66 chromophobe renal cell carcinomas (ChRCCs) based on multidimensional and comprehensive characterization, including mitochondrial DNA (mtDNA) and whole genome sequencing. The result is consistent that ChRCC originates from the distal nephron compared to other kidney cancers with more proximal origins. Combined mtDNA and gene expression analysis implicates changes in mitochondrial function as a component of the disease biology, while suggesting alternative roles for mtDNA mutations in cancers relying on oxidative phosphorylation. Genomic rearrangements lead to recurrent structural breakpoints within *TERT* promoter region, which correlates with highly elevated *TERT* expression and manifestation of kataegis, representing a mechanism of *TERT* up-regulation in cancer distinct from previously-observed amplifications and point mutations.

Introduction

Rare tumor types offer a unique opportunity to investigate and discover mechanisms of tumorigenesis. Chromophobe kidney cancer (ChRCC) is a subtype of renal cell carcinoma (RCC), representing ∼5% of this heterogenous group of cancers arising from the nephron (Storkel et al., 1997), with 3,000 new cases annually in the United States (Jemal et al., 2013). Although ChRCC typically exhibits an indolent pattern of local growth, with greater than 90% ten-year cancer-specific survival (Amin et al., 2002; Przybycin et al., 2011), aggressive features and metastasis can occur. ChRCC is associated with a distinct aneuploidy pattern (Speicher et al., 1994); however, genome-wide evaluation of its somatic mutation spectrum has not been reported. ChRCC is associated with germline mutation of *FLCN* in the autosomal dominant cancer predisposition Birt-Hogg-Dubé (BHD) syndrome, where 34% of BHD-associated kidney tumors are ChRCC (Nickerson et al., 2002; Pavlovich et al., 2002; Schmidt et al., 2001), and with germline mutation of *PTEN* in Cowden syndrome (Shuch et al., 2013). Previous studies have suggested a non-glycolytic metabolic profile for ChRCC, using F-18-fluorodeoxyglucose PET/CT (Ho et al., 2012), and have shown that the genomic profile comprises unique whole chromosome losses rather than focal events (Speicher et al., 1994).

Genomic profiling of rare cancers, such as ChRCC, can provide a more complete picture of the disease. Although very large sample numbers (>5000) may be needed for some disease types in order to detect rare mutational events (Lawrence et al., 2014), in many cases there

remain undiscovered frequent mutations that drive disease. When data integration across multiple platforms is applied, patterns observed in one data type may be reflected in the other data types, building a more conclusive set of findings with regard to revealing driver events. For example, early DNA microarray studies of breast cancer, e.g. globally assaying a single data type for 65 tumors (Perou et al., 2000) and incorporating clinical data, have had an enduring impact on our understanding of breast and other cancers, while *PBRM1* mutations were discovered in clear cell kidney cancers from an initial analysis of just 25 tumors (Varela et al., 2011). Understudied cancers, such as ChRCC, may hold this potential for discovery as well.

Results

Copy Number and Whole Exome Analysis

The Cancer Genome Atlas (TCGA) collected a total of 66 primary ChRCC specimens (Table S1) with matching normal tissue/blood, in order to better characterize the molecular basis of this cancer using multiple data platforms (Tables 1 and S1). Our comprehensive analysis of ChRCC involved a systematic examination by data type, including copy number and whole-exome sequencing (WES). By SNP array analysis, loss of one copy of the entire chromosome, for most or all of chromosomes 1, 2, 6, 10, 13, and 17, was seen in the majority of cases (86%, Figure 1A). Losses of chromosomes 3, 5, 8, 9, 11, 18, and 21 were also noted at significant frequencies (12-58%). There were no focal copy number events by GISTIC analysis (Mermel et al., 2011), suggestive of a simpler chromosomal landscape for ChRCC in comparison to that of other cancers, including the more common clear cell type RCC (ccRCC). We subdivided our ChRCC cases according to previously defined histologic categories of “classic” (n=47), which demonstrate the classical pale cytoplasmic features for which the disease was named, and “eosinophilic” (n=19), based on abundant, eosinophilic cytoplasm and densely packed mitochondria, by expert consensus pathology review (Brunelli et al., 2005). While all classic cases showed the characteristic ChRCC copy number pattern, only about half of the eosinophilic cases (10/19) showed the same, with four eosinophilic cases showing no copy number alterations. This suggests a degree of genomic heterogeneity that distinguishes the histopathology-based classifications.

WES of 66 ChRCC cases targeted ∼186,260 exons in ∼18,091 genes, achieving 90% target coverage at a minimum of 20X for both tumor and matched normal samples. Overall, ChRCC displayed a low median rate of exonic somatic mutations (∼0.4 per Mb) compared to most tumors (Alexandrov et al., 2013), approximately 3-fold less than the median number seen in ccRCC (which differences were also observable within strata defined by age or stage), with the one exception showing elevated somatic mutation rate (>10/Mb by WES) and mutation signature of DNA mismatch repair deficiency (Alexandrov et al., 2013). Using alternative sequencing instrumentation, we validated 60 somatic mutation events for a set of 30 genes both arising from WES and having inferred biologically relevance (Table S2). While our lower case numbers limited purely data-driven approaches to assigning statistical significance to infrequently mutated genes, we did have sufficient power to identify significant genes with a frequency of ∼10% (Lawrence et al., 2014). Only two significant genes were thus identified (MutSig q<0.1): *TP53* and *PTEN*.

TP53 was frequently mutated in 32% of cases (21 of the 66 profiled), with mutations correlating with decreased expression of p53 transcriptional targets (Figures S1A-S1C). *PTEN* was the next most frequently mutated, with 9% (6 of 66) nonsilent mutations detected. No other genes were found to be mutated at a frequency higher than 5%, though mutations involving cancer-relevant genes were found at lower frequencies (Figure 1B). Mutations were seen in *MTOR* (2 cases), *NRAS* (1 activating mutation), and *TSC1* or *TSC2* (4 cases), and two homozygous deletions were seen in *PTEN*, indicating that genomic targeting of the mTOR pathway occurred overall in 15 (23%) of 66 ChRCC (Figure 1B). Biological significance could be ascribed to infrequently mutated genes, in terms of associated pathways, including the p53 and PTEN pathways (Table S2). The genetic diseases BHD and TSC both predispose to the development of ChRCC, and associated mutations converge in activation of the PTEN signaling pathway. Our study focused on sporadic disease, and a surprisingly high percentage (∼47%) of our core cases did not show alterations associated with either PTEN or p53 pathways. As no additional pathways involving sizeable numbers of cases could be implicated from the exome data, our search was extended to mtDNA and structural variant analysis, as described below.

DNA Methylation and RNA Analysis

TCGA data platforms allow for comparisons between tumor types (Cancer_Genome_Atlas_Research_Network et al., 2013). For example, we observed widespread differences in DNA methylation between ChRCC and ccRCC (Figure 2A), involving over 64K loci out of ∼450K profiled ($p<0.001$, t-test using logit-transformed data, beta value difference>0.1). ChRCC displayed more hypomethylation and fewer hypermethylation events compared to ccRCC. We also observed epigenetic silencing of *CDKN2A*/p16 in four ChRCC cases (Figure 2B). In principle, differential DNA methylation patterns could involve cancer-relevant pathways, but may also reflect cell of origin of the cancer (Shen and Laird, 2013). Based on immunohistochemical analyses (Prasad et al., 2007), ChRCC has been postulated to arise from intercalated cells in the distal convoluted tubule of the nephron, while ccRCC is thought to arise from cells in the proximal convoluted tubule; however, this issue has remained unresolved. The above DNA methylation patterns were consistent with distinct origins, leading us to further explore these origins using gene expression data.

We examined our gene expression data in the context of an external gene expression dataset of normal tissue microdissected from various regions of the nephron (Cheval et al., 2012). Supervised analysis, globally comparing each TCGA ChRCC or ccRCC tumor expression profile (n=66 and n=417, respectively) to that of each sample in the nephron atlas, showed high mRNA expression correlations for ChRCC with distal regions of the nephron. ccRCC gene expression, however, was correlated with patterns associated with the proximal nephron (Figure 2C). These associations were also evident, when focusing on the subset of differential genes in ChRCC versus ccRCC associated with inverse DNA methylation changes (Figure 2D). These results put in context many of the widespread molecular differences between these two kidney cancer types, as well as suggesting that cancers may be defined in part by cell of origin in addition to genetic aberrations.

In addition to widespread differences in gene expression between ChRCC and ccRCC, and differences from normal kidney (Figure S2A and Table S3), unsupervised clustering of mRNA profiles indicated further molecular heterogeneity within ChRCC, with at least two subsets identified (Figure S2B) as defined by differential gene expression patterns. Cluster analysis of miRNA profiles also indicated heterogeneity (Figure S2C), and we could identify anti-correlations between miRNAs and their predicted mRNA targets (Table S4), including an anti-correlation (False Discovery Rate, or FDR<0.01) involving miR-145 (low in ChRCC versus normal) and the complex I-associated *NDUFA4* gene (Figure S2D)(Kano et al., 2010). Molecular correlates of patient survival in ChRCC were identifiable at levels of mRNA, miRNA, and DNA methylation (Table S5); many of these correlates were shared with those previously observed for ccRCC (The_Cancer_Genome_Atlas_Research_Network, 2013) and included cell cycle genes, but not the 'Warburg effect'-like patterns of aggressive ccRCC (The_Cancer_Genome_Atlas_Research_Network, 2013).

Pathway and Mitochondrial DNA Analysis

When viewed in the context of mitochondrial function, expression of nuclear-encoded genes in ChRCC, as compared to normal kidney, suggested increased utilization of the Krebs cycle and electron transport chain (ETC) for adenosine triphosphate (ATP) generation (Figures 3A, S3A, and S3B). In ChRCC, nearly all genes encoding enzymes in the Krebs cycle showed increased expression over normal, with the entry of pyruvate into the Krebs cycle via Acetyl CoA likely through the pyruvate dehydrogenase complex (PDC). Concordantly, all complexes of the ETC demonstrated mRNA increases in at least one gene. These patterns could reflect an increased level of mitochondrial biosynthesis, resulting in greater numbers of mitochondria within each tumor cell; this possibility is supported by both the increased expression of mitochondrial biogenesis regulator *PPARGC1A* ($p<1E-5$, t-test using log-transformed data, Table S3), and increased mitochondrial genome copy numbers (four times more on average in ChRCC versus normal kidney, Figures 3B and S3C). These findings interestingly parallel the eosinophilic histology observed in some ChRCC, corresponding to the high uptake of eosin by mitochondria. Eosinophilic ChRCC tumors share many features with the benign variant oncocytoma, which is also characterized by dense accumulations of mitochondria (Amin et al., 2008; Tickoo et al., 2000). Furthermore, the gene expression landscape appeared very different from that of ccRCC, where expression of genes involved in mitochondrial functions is strongly suppressed (Figure S3D) (The_Cancer_Genome_Atlas_Research_Network, 2013). These findings suggest that various bioenergetics strategies may support tumor growth, and that not all cancers necessarily seek to minimize their reliance upon oxidative phosphorylation (The_Cancer_Genome_Atlas_Research_Network, 2013).

Given the indicated prevalent role of mitochondria in ChRCC and the likelihood of rapid mitochondrial genome replication (Figure 3B), we sequenced mtDNA from 61 of our 66 ChRCC cases, using a Polymerase Chain Reaction (PCR)-based amplification approach (Table S6). In all, we identified 142 somatic mutation events (i.e. not present in the normal) at various levels of heteroplasmy (i.e. mixture with other variants), 75 of these residing within the commonly altered D-Loop non-coding region (Chatterjee et al., 2006). Thirty-five

mutation events (involving 27 cases) were present in over 50% of mtDNA copies in the tumor (>50% heteroplasmy) (Figure 4A). Human mtDNA encodes 13 proteins involved in respiration and oxidative phosphorylation (Figure 3A), and we found 15 nonsilent mutations in 12 ChRCC cases involving these genes (>50% heteroplasmy), all of which validated using alternative strategies, including WGS-based analysis (Larman et al., 2012)(Table S6). Based on previous functional studies in oncocytoma (Gasparre et al., 2008; Mayr et al., 2008; Simonnet et al., 2003), and as many of our variants represented frameshift substitutions, these mtDNA mutations are thought, in general, to lead to inactivation, rather than activation, of the associated protein.

Electron transport chain Complex I genes were altered in 18% of cases (n=11, Figures 3A and 1B and Table S3); the most frequently altered gene was *MT-ND5*, in six cases (all with >70% heteroplasmy), with five of these being histologically classified as eosinophilic ChRCC ($p<0.01$, one-sided Fisher's exact test), and three showing no copy number abnormalities ($p<0.002$). *MT-ND5* is essential for the activity of complex I (Chomyn, 2001), which is responsible for the transfer of electrons from NADH to ubiquinone. One ChRCC case had a single base insertion at position 12417 that changes the length of an 8-bp homopolymer tract in *MT-ND5*, which has been observed previously in several other cancer types (Larman et al., 2012); another case had insertion at 12384, at which position a mutation was found elsewhere in oncocytoma and associated with loss of complex I activity (Mayr et al., 2008). Two ChRCC cases each had single base deletions at position 13230 of *MT-ND5*, but no other mtDNA mutations were recurrent in our cases. We also found *MT-ND5*-mutated ChRCC cases to have a distinct gene transcription signature (Figures 4B, S4A, and S4B, 719 genes with $p<0.001$ by t-test, FDR<0.05), which was shared by other eosinophilic cases and were not limited to genes in regions of recurrent copy number abnormality (Figure S4C). Genes with high expression in *MT-ND5*-mutated cases were enriched for those associated with mitochondria (43 with Gene Ontology term “mitochondrion”, $p<5E-6$, one-sided Fisher's exact test), including several with roles in ETC (*SDHB*, *NDUFS1*, *ATP5F1*, *COX10*, *COX11*, Table S3). Notably, mutations in complex I did not result in expression patterns associated with loss of oxidative phosphorylation (Figure 4C), as might be assumed (Larman et al., 2012), suggesting possible alternative roles for complex I alteration in cancer-associated metabolic activity (Figure S4D). The associations made here, involving mtDNA mutations with mitochondrial abundance and differential gene expression patterns (which may be unique to ChRCC and related cancers), could perhaps suggest either a compensatory role for loss of complex I function, or selective pressures operating to promote alternative pathways.

Whole Genome Analysis

WGS for 50 of our 66 ChRCC cases was performed (60X and 30X coverage for paired tumor and normal, respectively). Meerkat algorithm (Yang et al., 2013) was applied to detect genomic rearrangements, with an average of 16 found per case (range 0-207, Figure S5A), but without involving recurrent gene-gene fusions. By WGS analysis, a subset of ChRCC manifested kataegis (Figures 5A and S5B), a phenomenon involving highly localized substitution mutations (C>T or C>G). Consistent with observations in other cancers (Alexandrov et al., 2013; Nik-Zainal et al., 2012), we found that regions of kataegis

in ChRCC were found in the vicinity of genomic rearrangements (Figures 5A and S5B, average of 150 rearrangements by pter/qter region). Three ChRCC WGS profiles showed particularly strong patterns involving chromosomal regions 3p, 5p, 5q, 8q, 13q, or 15q (Figure 5B). A mutation signature consistent with APOBEC cytidine deaminase activity (Alexandrov et al., 2013; Roberts et al., 2013) was significantly enriched in kataegis regions as well as in tightly spaced mutation clusters forming kataegis events (Figures S5C-S5F, Table S7). While not detectable in ChRCC WES data (Alexandrov et al., 2013), WGS mutation spectra of six ChRCC cases, including the three with strong kataegis patterns, showed statistically significant (albeit moderate) APOBEC-patterned mutagenesis across the entire genome (Figure S5C). *APOBEC3B* mRNA expression was also elevated in ChRCC compared to normal kidney (Figure S5G).

We compared gene expression profiles between ChRCC cases with and without a strong kataegis pattern (n=3 and n=47, respectively), and identified 29 differentially expressed genes (FDR<0.05) including *TERT* (p<1E-10, t-test, FDR<1E-6, Figure 5C). The *TERT* gene itself showed a wide range of expression levels across ChRCC, from undetectable to hundreds of units by RNA-seq. Focusing our attention on *TERT*, we sequenced the promoter region for recently identified mutations (C228T and C250T) (Huang et al., 2013); three cases harbored C228T mutations, but were associated with only marginal *TERT* expression levels (average expression ∼1 unit). WGS analysis of DNA copy within the *TERT* region identified some copy number variation, but not at levels that would account for the extent of deregulated expression. However, multiple cases did show abrupt changes in copy number, at points that fell within the region 10 kb upstream of the *TERT* transcription start site (Figure 5D). This observation suggested the existence of structural breakpoints, leading us to reexamine our Meerkat-generated results with greater scrutiny.

Subsequent WGS analysis identified genomic rearrangements involving the *TERT* promoter region, leading to breakpoints within the region in six out of 50 ChRCC cases (Figure 5D and Table 2); these cases also had the highest levels of *TERT* expression (average>500 units, p<1E-20, t-test; Table 2 and Figure 5E), even compared to cases with 228T mutation, and three showed the strongest manifestation of kataegis (p=0.001, one-sided Fisher's exact). In five ChRCC cases, the *TERT*-associated rearrangements were intrachromosomal (one involving part of *PDCD6*), while the sixth case involved *NEK5* on chromosome 13. When considering intra-tumor heterogeneity, in most cases these variants were estimated to reside in nearly all of the cells (when counting the numbers of concordant versus discordant read pairs), which would indicate that the *TERT*-associated rearrangements represent early events and therefore possible drivers. Of the seven rearrangements identified by WGS, we confirmed six (involving six cases) by PCR, by designing primers that spanned both sides of the breakpoint junction (Figure 6A and Table S8), allowing for amplification of DNA spanning the breakpoint region in the tumor sample (Figures 6B and S6); subsequent sequencing of the PCR product independently confirmed the junction in each case (Figure 6C). While point mutations in the *TERT* promoter, leading to up-regulation of *TERT* itself, have been recently reported in cancers such as melanoma (Heidenreich et al., 2013; Huang et al., 2013), our results represent another phenomenon, of recurrent genomic rearrangement breakpoints in the *TERT* promoter being associated with elevated *TERT* expression in

cancer. A precise mechanism remains to be elucidated, though, as a result of rearrangement, a number of cis-regulatory elements were found to be placed in close proximity to the core promoter of *TERT* (Figure S7).

Discussion

With this comprehensive molecular survey of ChRCC, we have made several important findings, in particular the observed recurrent genomic structural rearrangements involving the *TERT* promoter region and elevated *TERT* expression, and our results raise intriguing questions regarding cancer, involving the role of mtDNA alterations and the role of the cell of origin. The above key findings were made possible only by our comprehensive approach, where, for example, we had no prior hypotheses regarding *TERT* at the onset of our study. Additionally, mtDNA mutations in cancer, particularly those involving *MT-ND5* and complex I, have been hypothesized elsewhere to recapitulate the Warburg effect (Larman et al., 2012), though the corresponding expression and histological patterns observed in our data were consistent with a complex metabolic phenotype rather than simple loss of oxidative phosphorylation. Taken together, our key findings further illustrate the need to survey cancers outside of exome boundaries, e.g. by incorporating WGS or mtDNA sequencing as part of an integrative, multi-platform analysis.

Through integration of molecular data from less common cancers, we can learn more about more frequently encountered diseases. Here, for example, our analysis of ChRCC led to additional insights regarding ccRCC. RCC represents a collection of highly distinct tumors arising from different lineages within the nephron, with distinct molecular and genetic features reflecting independent processes of tumorigenesis (Linehan, 2012). Given the complexity of function assigned to an organ such as the kidney, different cancers arising from this organ may not necessarily appear similar to each other (Alexandrov et al., 2013; The_Cancer_Genome_Atlas_Network, 2012). Our multi-platform analyses clearly confirm that ChRCC is a distinct disease entity from, and shares little cell lineage or genomic characteristics with, ccRCC, further reinforcing the notion that disease-specific therapies are needed for rarer tumors such as ChRCC, rather than simply adopting conventional therapeutic strategies used for ccRCC. Given the clear genetic differences between ChRCC and ccRCC, our results would suggest cell of origin as a key factor in disease determination, observations that could inform future efforts to fractionate the pool of susceptible cells for ChRCC or ccRCC modeling or preventative interventions. In addition, these data will serve as a resource for future explorations of other tumors of kidney origin, such as papillary renal cell carcinomas, while being broadly relevant as well to the study of other cancers, as metabolic, genomic structural alterations, and cellular factors that influence the spectrum of genetic events contributing to cancer development are further realized.

The gene expression patterns, increased mitochondrial numbers, and histological patterns associated with ChRCC all indicate an increased importance of a distinct mitochondrial respiration program in this disease. Renal oncocytoma, a benign renal tumor that, like ChRCC, may also arise from the distal nephron, shares several similarities with ChRCC (particularly with its eosinophilic subtype), including abundant, eosinophilic cytoplasm and densely packed mitochondria (Amin et al., 2008; Tickoo et al., 2000). Mitochondrial

accumulation in renal oncocytomas has been hypothesized to be a compensatory mechanism for inefficient oxidative phosphorylation (Simonnet et al., 2003), where loss of complex I activity may result from somatically acquired homoplasmic mutations in mitochondrial complex I genes (Gasparre et al., 2008; Mayr et al., 2008; Simonnet et al., 2003). However, gene expression in ChRCC would indicate that increased oxidative phosphorylation is maintained in complex I-altered tumors, suggesting a metabolic shift supporting the growth of this tumor, and counter to the Warburg-like phenomenon observed in high grade, high stage ccRCC and many other cancers (The_Cancer_Genome_Atlas_Research_Network, 2013), which would appear consistent with previous observations, using metabolic imaging to demonstrate uptake of radiolabeled acetate but not glucose in ChRCC (Ho et al., 2012). In general, cancer cells derive much of their ATP through oxidative phosphorylation (Ward and Thompson, 2012), and cancer-associated reprogramming of mitochondria and of other metabolic pathways, besides glycolysis and the Warburg effect, have recently received much attention (Currie et al., 2013; Ward and Thompson, 2012). Further studies to dissect the precise role of mtDNA alterations in cancer, and mitochondrial activities promoting cancer growth, could shed light on how core metabolic pathways may be altered in ChRCC and other malignant diseases.

Our finding of recurrent DNA rearrangement breakpoints within the *TERT* promoter region in over 10% of evaluated cases represents a mechanism for increased *TERT* expression in cancer different from point mutations observed in a wide variety of cancers (Heidenreich et al., 2013; Huang et al., 2013), gene amplification (Weir et al., 2007; Y et al., 2005), and germline polymorphisms (Rafnar et al., 2009). *TERT* is well-recognized as having roles in telomere maintenance and DNA repair, where deregulation of telomerase is a ubiquitous feature of human cancers. The previously-observed *TERT* promoter mutations (C228T and C250T) create *de novo* E-twenty six/ternary complex factors (Ets/TCF) binding sites, which have been observed to increase transcriptional activity from the promoter by two-to fourfold (Huang et al., 2013). Interestingly, the *TERT* expression levels of the six cases with independently validated *TERT* promoter rearrangements were much higher than those cases with C228T promoter mutations, suggesting that these rearrangements might have an even more potent effect on up-regulation of the gene. The precise mechanism of how these rearrangements affect expression remains to be elucidated; they could possibly involve rearranged cis-regulatory elements or could allow the core *TERT* promoter to escape from the native condensed chromatin environment (Zhao et al., 2009). The observed association of *TERT* with kataegis is also intriguing. Elsewhere, rearrangement of DNA sequences upstream of *TERT* have been reported in immortalized, non-tumorigenic fibroblasts, leading to activated telomerase in cells surviving the crisis stage of immortalization (Zhao et al., 2009), which involves chromosomal instability and rearrangements due to loss of telomere capping activity; in the setting of human cancer, this would suggest that *TERT*-associated rearrangements would be involved in many cases at an early stage in tumorigenesis.

Future applications of the information presented here will include comparative analysis with other cancer types, for the possible existence elsewhere of structural rearrangements involving promoters for *TERT* or for other key drivers. As a resource with a large set of whole genome sequences, integrated with a broad array of high quality platform datasets,

other relationships between genomic structural alterations and transcriptional components, including noncoding RNAs, remain to be uncovered. As our data represent single biopsies, future studies might focus on heterogeneity between biopsies from the same tumor (Gerlinger et al., 2012); additionally, sub-clonal analysis may shed light on early vs late somatic events in ChRCC tumorigenesis. Our study also revealed that divergent approaches for uncovering mtDNA mutations (long-range PCR versus WGS (Larman et al., 2012)) are highly complementary to each other, allowing WGS data from other cancers to be similarly mined for mtDNA mutations, with the additional step of combining these data with that of other platforms, in order to better understand the role of the mitochondria in cancer. Finally, the underlying datasets presented here represent part of an interlocking toolset, that can be combined with those of other cancers (Cancer_Genome_Atlas_Research_Network et al., 2013), for further discovery of driver alterations, both within and beyond the exome.

Experimental Procedures

Patient and Sample Characteristics

With informed consent, biospecimens were collected from newly diagnosed patients with ChRCC undergoing surgical resection and who had received no prior treatment for their disease. Samples were obtained with approval from institutional review boards at Brigham and Women's Hospital, Memorial Sloan-Kettering Cancer Center, National Cancer Institute, and The University of Texas M.D. Anderson Cancer Center. Using a co-isolation protocol, DNA and RNA were purified. Details of sample preparation are described in the Supplemental Experimental Procedures.

Data Generation

In total, 66 ChRCC cases were assayed on at least one molecular profiling platform (Table 1), which platforms included: (1) RNA sequencing; (2) DNA methylation arrays; (3) miRNA sequencing; (4) Affymetrix SNP arrays; (5) whole exome sequencing; (6) whole genome sequencing; and (7) mtDNA sequencing (using long-range PCR to amplify mtDNA). As described above and in the Supplemental Experimental Procedures, both single platform analyses and integrated cross-platform analyses were performed. Sequence files are available from CGHub (https://cghub.ucsc.edu/). All other molecular, clinical and pathological data are available through the TCGA Data Portal (https://tcga-data.nci.nih.gov/tcga/).

Whole-Genome and Exome Sequencing Analysis

Massively Parallel Sequencing Exome capture was performed using NimbleGen (custom designed) VCRome 2.1 (42MB) according the manufacturer's instructions. All exome and whole-genome sequencing was performed on the Illumina HiSeq platforms. Basic alignment and initial sequence analysis were carried out using the Mercury analysis pipeline (Reid et al., 2014).

MtDNA Sequencing Analysis

MtDNA was isolated from tissue samples using long-range PCR methods. Amplified mtDNA PCR products were constructed into Illumina paired-end libraries, and raw sequence data were pre-processed and aligned using the Mercury pipeline.

RNA Sequencing Analysis

Both mRNA and miRNA libraries were separately generated from total RNA and constructed using manufacturer protocols. Sequencing was done on the Illumina HiSeq platform. Read mapping and downstream data analysis were performed as described in the Supplemental Experimental Procedures.

Array Data Analysis

DNA was hybridized to Affymetrix SNP 6.0 arrays and Illumina Infinium HumanMethylation450 (HM450) BeadChip arrays, according to manufacturer protocols.

Supplementary Material

Refer to Web version on PubMed Central for supplementary material.

Acknowledgments

We wish to thank all patients and families who contributed to this study. This work was supported by the following grants from the USA National Institutes of Health (NIH): 5U24CA143843 (D. Wheeler), U54HG003273 (R. Gibbs), NIH R01GM103502-05 (G. Roberston); KL2TR001109 and UL1TR001111 (A. Smith), 5P50CA101942 (S. Signoretti), 5P50CA101942 (T. Choueiri), U54 HG003067 (E. Lander). Intramural Research Program of the NIH, National Cancer Institute, Center for Cancer Research (W.M. Linehan, L.S. Schmidt, C.J. Ricketts, M.J. Merino), with Federal funds from the Frederick National Lab, NIH, under contract HHSN261200800001E (L.S. Schmidt), Intramural Research Program of the NIH, National Institute of Environmental Health Sciences (D.A. Gordenin, S.A. Roberts, L.J. Klimczak, D. Fargo), and a training fellowship from the Keck Center for Interdisciplinary Bioscience Training of the Gulf Coast Consortia (Grant No. T15 LM007093, C.F. Davis). Other grant support includes: the J. Randall & Kathleen L. MacDonald Kidney Cancer Research Fund, the Tuttle Family Kidney Cancer Research Fund (J. Hsieh), the Korean Health Technology R&D Project, Ministry of Health & Welfare, Republic of Korea (HI13C2096, W-Y. Park), and the Korea Institute of Science and Technology Information (KISTI): K-14-L01-C02-S04, KSC-2013-C3-037 (for supercomputing resources including technical support).

TCGA Consortium

Analysis Working Group

Baylor College of Medicine – Chad J. Creighton(1, 2), Caleb F. Davis(1), Margaret Morgan(1), Preethi H. Gunaratne(1, 3), Lawrence A. Donehower(1), Benny A. Kaipparettu(2, 4), David A. Wheeler(1), Richard A. Gibbs(1), *Brigham and Women's Hospital* – Sabina Signoretti(5, 6), *Broad Institute* – Andrew D. Cherniack(7), *Canada's Michael Smith Genome Sciences Centre BC Cancer Agency* – A. Gordon Robertson(8), Andy Chu(8), *Dana Farber Cancer Institute* - Toni K. Choueiri(6, 9), Elizabeth P. Henske(6, 7, 9), David J. Kwiatkowski(6, 7, 9), *Memorial Sloan-Kettering Cancer Center* – Victor Reuter(10), James J. Hsieh(11, 12), A. Ari Hakimi(13), Satish K. Tickoo(10), *National Cancer Institute* -Christopher Ricketts(14), W. Marston Linehan(14), Laura S. Schmidt(14, 15), *National Institute of Environmental Health Sciences* – Dmitry A.

Gordenin(16), *Rutgers University* – Gyan Bhanot(17, 18), Michael Seiler(19), *The University of Texas M.D. Anderson Cancer Center* - Pheroze Tamboli(20), *University of North Carolina, Chapel Hill* - W. Kimryn Rathmell(21-23), Catherine C. Fahey(24), Kathryn E. Hacker(24), Angela B. Smith(23), Eric M. Wallen(23), *University of Southern California* – Hui Shen(25), Peter W. Laird(25), *Yale University* – Brian Shuch(26).

Genome Sequencing Center

Baylor College of Medicine - Donna Muzny(1), Caleb F. Davis(1), Christian Buhay(1), Min Wang(1), Margaret Morgan(1), Lawrence A. Donehower(1), Hsu Chao(1), Mike Dahdouli(1), Liu Xi(1), Nipun Kakkar(1), Jeffrey G. Reid(1), Brittany Downs(1), Jennifer Drummond(1), Donna Morton(1), Harsha Doddapaneni(1), Lora Lewis(1), Adam English(1), Qingchang Meng(1), Christie Kovar(1), Qiaoyan Wang(1), Walker Hale(1), Alicia Hawes(1), Divya Kalra(1), Kimberly Walker(1), Chad J. Creighton(1, 2), David A. Wheeler(1), Richard A. Gibbs(1).

Genome Characterization Centers

Broad Institute – Andrew D. Cherniack(7), Bradley A. Murray(7), Carrie Sougnez (7), Gordon Saksena(7), Scott L. Carter(7), Steven E. Schumacher(7, 27), Barbara Tabak(7, 27), Travis I. Zack(7, 27), Gad Getz(7, 28), Rameen Beroukhim(6, 7, 9, 27), Stacey B. Gabriel(7), Matthew Meyerson(6, 7, 29), *Canada's Michael Smith Genome Sciences Center, BC Cancer Agency* – Adrian Ally(8), Miruna Balasundaram(8), Inanc Birol(8), Denise Brooks(8), Yaron S.N. Butterfield(8), Andy Chu(8), Eric Chuah(8), Amanda Clarke(8), Noreen Dhalla(8), Ranabir Guin(8), Robert A. Holt(8), Katayoon Kasaian(8), Darlene Lee(8), Haiyan I. Li(8), Emilia Lim(8), Yussanne Ma(8), Michael Mayo(8), Richard A. Moore(8), Andrew J. Mungall(8), A. Gordon Robertson(8), Jacqueline E. Schein(8), Payal Sipahimalani(8), Angela Tam(8), Nina Thiessen(8), Tina Wong(8), Steven J.M. Jones(8), Marco A. Marra(8), *University of North Carolina, Chapel Hill* - J. Todd Auman(30), Donghui Tan(21), Shaowu Meng(31), Corbin D. Jones(32, 33), Katherine A. Hoadley(31), Piotr A. Mieczkowski(21), Lisle E. Mose(31), Stuart R. Jefferys(31), Jeffrey Roach(34), Umadevi Veluvolu(21), Matthew D. Wilkerson (31), Scot Waring(21), Elizabeth Buda(33), Junyuan Wu(31), Tom Bodenheimer(31), Alan P. Hoyle(31), Janae V. Simons(31), Mathew G. Soloway(31), Saianand Balu(31), Joel S. Parker(21, 31), D. Neil Hayes(31, 35), Charles M. Perou(21, 31, 36), *University of Southern California & Johns Hopkins* – Hui Shen(25), Daniel J. Weisenberger(25), Moiz S. Bootwalla(25), Timothy Triche Jr. (25), Phillip H. Lai(25), David J. Van Den Berg(25), Stephen B. Baylin(37), Peter W. Laird(25).

Genome Data Analysis

Baylor College of Medicine – Chad J. Creighton(1, 2), Fengju Chen(2), Cristian Coarfa(2, 38), Caleb F. Davis(1), Lawrence A. Donehower(1), Preethi H. Gunaratne(1, 3), David A. Wheeler(1), *Broad Institute* - Gad Getz(7, 28), Michael S. Noble(7), Daniel DiCara(7), Hailei Zhang(7), Juok Cho(7), David I. Heiman(7), Nils Gehlenborg(7), Gordon Saksena(7), Doug Voet(7), Pei Lin(7), Scott Frazer(7), Petar Stojanov(6, 7), Yingchun Liu(7), Lihua Zou(7), Jaegil Kim(7), Michael S. Lawrence(7), Lynda Chin(7, 39), *Harvard Medical*

School/The University of Texas M.D. Anderson Cancer Center - Lixing Yang(40), Sahil Seth(39), Christopher A. Bristow(39), Alexei Protopopov(39), Xingzhi Song(39), Jianhua Zhang(39), Angeliki Pantazi(41), Angela Hadjipanayis(41), Eunjung Lee(40), Lovelace J. Luquette(40), Semin Lee(40), Michael Parfenov(41), Netty Santoso(41), Jonathan Seidman(41), Andrew W. Xu(40), Lynda Chin(7, 39), Raju Kucherlapati(41, 42), Peter J. Park(40, 41), *Korea Institute of Science and Technology Information* – Hyojin Kang(43), Junehawk Lee(43, 44), *National Institute of Environmental Health Sciences*– Dmitry A. Gordenin(16), Steven A. Roberts(16), Leszek J. Klimczak(16), David Fargo(16), *National Institutes of Health* – Martin Lang(14), *Rutgers University* – Gyan Bhanot(17, 18), Michael Seiler(19), *Samsung Genome Institute* – Yoon-La Choi(45), Sang Cheol Kim(45), June-Koo Lee(46), Woong-Yang Park(45, 47), *The University of Texas M.D. Anderson Cancer Center* – Wenyi Wang(48), Yu Fan(48), Jaeil Ahn(48), Rehan Akbani(48), John N. Weinstein(48), *UC Santa Cruz* -David Haussler(49, 50), Singer Ma(50), Amie Radenbaugh(50), Jingchun Zhu(50), *University of Groningen* – Michael Biehl(51), *University of Houston* – Preethi H. Gunaratne(1, 3).

Biospecimen Core Resource

The Research Institute at Nationwide Children's Hospital - Tara M. Lichtenberg(52), Erik Zmuda(52), Aaron D. Black(52), Benjamin Hanf(52), Nilsa C. Ramirez(52, 53), Lisa Wise(52), Jay Bowen(52), Kristen M. Leraas(52), Tracy M. Hall(52), Julie M. Gastier-Foster(52, 53).

Tissue Source Sites

Brigham and Women's Hospital - Sabina Signoretti(5, 6), *Dana-Farber Cancer Institute* – William G. Kaelin(6, 9), Toni K. Choueiri(6, 9), *Memorial Sloan-Kettering Cancer Center* - Satish K. Tickoo(10), Victor Reuter(10), A. Ari Hakimi(13), *University of North Carolina at Chapel Hill* - W. Kimryn Rathmell(21-23), Leigh Thorne(31), Lori Boice(31), Mei Huang(31), *National Cancer Institute* - W. Marston Linehan(14), Cathy Vocke(14), James Peterson(14), Robert Worrell(14), Maria Merino(14), Laura S. Schmidt(14, 15), *The University of Texas M.D. Anderson Cancer Center* – Pheroze Tamboli(20), Bogdan A. Czerniak(20), Kenneth D. Aldape(20), Christopher G. Wood(54).

Disease Working Group

Baylor College of Medicine – Richard A. Gibbs(1), Margaret Morgan(1), David A. Wheeler(1), *Brigham and Women's Hospital* - Sabina Signoretti(5, 6), *Oregon Health and Sciences University* – Paul T. Spellman(55), *Dana-Farber Cancer Institute* - Toni K. Choueiri (6, 9), William G. Kaelin(6, 9), *Georgetown University* - Michael B. Atkins(56), *Memorial Sloan-Kettering Cancer Center* - Satish K. Tickoo(10), Victor Reuter(10), *National Cancer Institute* - W. Marston Linehan(14), Cathy Vocke(14), Maria Merino(14), Laura S. Schmidt(14, 15), *The University of Texas M.D. Anderson Cancer Center* -Pheroze Tamboli(20), Christopher G. Wood(54), Kenneth D. Aldape(20), *Mayo Clinic* – John Cheville(57), R. Houston Thompson(57), *University of North Carolina, Chapel Hill* - W. Kimryn Rathmell(21-23), *Broad Institute* – Rameen Beroukhim(6, 7, 9, 27).

Data Coordination Center

SRA International - Mark A. Jensen(58), Todd Pihl(58), Yunhu Wan(58), Brenda Ayala(58), Julien Baboud(58), Sudhakar Velaga(58), Jessica Walton(58), Yunhu Wan(58), *SAIC-Frederick Inc.* – Jia Liu(59), Sudha Chudamani(59), Ye Wu(59).

Project Team

National Cancer Institute - Margi Sheth(60), Kenna R. Mills Shaw(60, 61), John A. Demchok(60), Tanja Davidsen(60), Liming Yang(60), Zhining Wang(60), Roy W. Tarnuzzer(60), Jiashan Zhang(60), Greg Eley(60), Ina Felau (49), Jean Claude Zenklusen(60), *National Human Genome Research Institute* -Carolyn M. Hutter(62), Mark S. Guyer(62), Bradley A. Ozenberger(62), Heidi J. Sofia(62), *Scimentis, LLC* - Greg Eley(63).

1. Human Genome Sequencing Center, Baylor College of Medicine, Houston, TX 77030.

2. Dan L. Duncan Cancer Center, Baylor College of Medicine, Houston, TX 77030.

3. Department of Biology & Biochemistry, University of Houston, 4800 Calhoun Road, Houston, TX 77204.

4. Department of Molecular and Human Genetics, Baylor College of Medicine, Houston, TX 77030, USA.

5. Department of Pathology, Brigham and Women's Hospital, 75 Francis Street, Boston MA 02115.

6. Department of Medical Oncology, Dana-Farber Cancer Institute, 450 Brookline Ave, Boston, MA 02215.

7. The Eli and Edythe L. Broad Institute of Massachusetts Institute of Technology and Harvard University, Cambridge, MA 02142.

8. Canada's Michael Smith Genome Sciences Centre, BC Cancer Agency, Vancouver, BC V5Z 4S6.

9. Department of Medicine, Harvard Medical School, Boston, MA 02215.

10. Department of Pathology, Memorial Sloan-Kettering Cancer, 1275 York Avenue, New York, NY 10065.

11. Department of Medicine, Weill-Cornell Medical College, New York, NY 10021.

12. Human Oncology and Pathogenesis Program, Memorial Sloan-Kettering Cancer Center, New York, NY 10065.

13. Department of Surgery, Urology Service Memorial Sloan Kettering Cancer Center, New York, NY 10065.

14. Urologic Oncology Branch, Center for Cancer Research, National Cancer Institute CRC Room 1W-5940 Bethesda, MD 20892.

15. Leidos Biomedical Research, Inc., Basic Science Program, Frederick National Laboratory for Cancer Research, Frederick, MD 21702.

16. National Institute of Environmental Health Sciences, 111 T.W. Alexander Drive, Research Triangle Park, NC 27709.

17. Department of Molecular Biology and Biochemistry, Rutgers University, Busch Campus, Piscataway, NJ 08854.

18. Cancer Institute of New Jersey, 195 Little Albany Street, New Brunswick, NJ 08903.

19. Bioinformatics Program, Boston University, 24 Cummington St, Boston, MA 02215.

20. Department of Pathology, The University of Texas, M.D. Anderson Cancer Center, 1515 Holcombe Boulevard, Houston, TX 77030.

21. Department of Genetics, University of North Carolina at Chapel Hill, NC 27599.

22. Department of Medicine, Division of Hematology and Oncology, University of North Carolina, Chapel Hill, NC 27599.

23. Department of Urology, University of North Carolina, Chapel Hill, NC 27599.

24. Curriculum in Genetics and Molecular Biology, Lineberger Comprehensive Cancer Center, University of North Carolina, Chapel Hill, NC 27599.

25. USC Epigenome Center, University of Southern California, Los Angeles, CA 90033.

26. Department of Urology, Yale School of Medicine, New Haven, CT 06520.

27. Department of Cancer Biology, Dana-Farber Cancer Institute, Boston, MA 02215.

28. Massachusetts General Hospital Cancer Center and Department of Pathology, Massachusetts General Hospital and Harvard Medical School, Boston, MA 02114.

29. Department of Pathology, Harvard Medical School, Boston, MA 02215.

30. Eshelman School of Pharmacy, University of North Carolina at Chapel Hill, Chapel Hill, NC 27599.

31. Lineberger Comprehensive Cancer Center, University of North Carolina at Chapel Hill, Chapel Hill, NC 27599.

32. Department of Biology, University of North Carolina at Chapel Hill, Chapel Hill, NC 27599.

33. Carolina Center for Genome Sciences, University of North Carolina at Chapel Hill, Chapel Hill, NC 27599.

34. Research Computing Center, University of North Carolina at Chapel Hill, Chapel Hill, NC 27599.

35. Department of Internal Medicine, Division of Medical Oncology, University of North Carolina at Chapel Hill, Chapel Hill, NC 27599

36. Department of Pathology and Laboratory Medicine, University of North Carolina at Chapel Hill, NC 27599.

37. Cancer Biology Division, The Sidney Kimmel Comprehensive Cancer Center at Johns Hopkins University, Baltimore, Maryland 21287.

38. Department of Molecular and Cellular Biology, Baylor College of Medicine, Houston, TX 77030.

39. Institute for Applied Cancer Science, Department of Genomic Medicine, The University of Texas MD Anderson Cancer Center, Houston, TX 77030.

40. Center for Biomedical Informatics, Harvard Medical School, Boston, MA 02115.

41. Department of Genetics, Harvard Medical School, Boston, MA 02115.

42. Division of Genetics, Brigham and Women's Hospital, Boston, MA 02115.

43. National Institute of Supercomputing and Networking, Korea Institute of Science and Technology Information, Daejeon, Korea.

44. Department of Bio and Brain Engineering, Korea Advanced Institute of Science and Technology, Daejeon, Korea.

45. Samsung Genome Institute, Samsung Medical Center, Seoul, Korea.

46. Graduate School of Medical Science and Engineering, Korea Advanced Institute of Science and Technology, Daejeon, Korea.

47. Sungkyunkwan University School of Medicine, Seoul, Korea.

48. Department of Bioinformatics and Computational Biology, The University of Texas MD Anderson Cancer Center, Houston, TX 77030.

49. Howard Hughes Medical Institute, University of California Santa Cruz, Santa Cruz, CA 95064.

50. Department of Biomolecular Engineering and Center for Biomolecular Science and Engineering, University of California Santa Cruz, Santa Cruz, CA 95064.

51. University of Groningen, Johann Bernoulli Institute for Mathematics and Computer Science, Intelligent Systems Group, P.O. Box 407, 9700 AK Groningen.

52. The Research Institute at Nationwide Children's Hospital, Columbus, OH 43205.

53. The Ohio State University, Columbus, OH 43210.

54. Department of Urology, The University of Texas MD Anderson Cancer Center, Houston, TX 77030.

55. Oregon Health and Science University, Department of Molecular and Medical Genetics, Portland, OR 97239.

56. Georgetown-Lombardi Comprehensive Cancer Center, Georgetown University, Washington D.C. 20057.

57. Mayo Clinic, Rochester, MN 55905.

58. SRA International, Inc., 4300 Fair Lakes Court, Fairfax, VA 22033.

59. SAIC-Frederick, Inc., 1050 Boyles Street, Frederick, MD 21702.

60. National Cancer Institute, 31 Center Dr, 3A20, Bethesda, MD 20892.

61. The MD Anderson Cancer Center Sheikh Khalifa Bin Zayed Al Nahyan Institute for Personalized Cancer Therapy (IPCT) 1400 Holcombe Blvd, FC12.2002 Houston, TX 77030.

62. National Human Genome Research Institute, National Institutes of Health, 5635 Fishers Lane, Bethesda, MD 20892.

63. Scimentis, LLC, Atlanta, GA 30666.

Reference List

Alexandrov LB, Nik-Zainal S, Wedge DC, Aparicio SA, Behjati S, Biankin AV, Bignell GR, Bolli N, Borg A, Borresen-Dale AL, et al. Signatures of mutational processes in human cancer. Nature. 2013; 500:415–421. [PubMed: 23945592]

Amin MB, Amin MB, Tamboli P, Javidan J, Stricker H, de-Peralta Venturina M, Deshpande A, Menon M. Prognostic impact of histologic subtyping of adult renal epithelial neoplasms: an experience of 405 cases. Am J Surg Pathol. 2002; 26:281–291. [PubMed: 11859199]

Amin MB, Paner GP, Alvarado-Cabrero I, Young AN, Stricker HJ, Lyles RH, Moch H. Chromophobe renal cell carcinoma: histomorphologic characteristics and evaluation of conventional pathologic prognostic parameters in 145 cases. Am J Surg Pathol. 2008; 32:1822–1834. [PubMed: 18813125]

Brunelli M, Eble JN, Zhang S, Martignoni G, Delahunt B, Cheng L. Eosinophilic and classic chromophobe renal cell carcinomas have similar frequent losses of multiple chromosomes from among chromosomes 1, 2, 6, 10, and 17, and this pattern of genetic abnormality is not present in renal oncocytoma. Modern pathology : an official journal of the United States and Canadian Academy of Pathology, Inc. 2005; 18:161–169.

Weinstein J, Collisson E, Mills G, Shaw K, Ozenberger B, Ellrott K, Shmulevich I, Sander C, Stuart J. Cancer_Genome_Atlas_Research_Network. The Cancer Genome Atlas Pan-Cancer analysis project. Nature genetics. 2013; 45:1113–1120. [PubMed: 24071849]

Chatterjee A, Mambo E, Sidransky D. Mitochondrial DNA mutations in human cancer. Oncogene. 2006; 25:4663–4674. [PubMed: 16892080]

Cheval L, Pierrat F, Rajerison R, Piquemal D, Doucet A. Of mice and men: divergence of gene expression patterns in kidney. PloS one. 2012; 7:e46876. [PubMed: 23056504]

Chomyn A. Mitochondrial genetic control of assembly and function of complex I in mammalian cells. J Bioenerg Biomembr. 2001; 33:251–257. [PubMed: 11695835]

Currie E, Schulze A, Zechner R, Walther TC, Farese RVJ. Cellular fatty acid metabolism and cancer. Cell Metab. 2013; 18:153–161. [PubMed: 23791484]

Gasparre G, Hervouet E, de Laplanche E, Demont J, Pennisi LF, Colombel M, Mege-Lechevallier F, Scoazec JY, Bonora E, Smeets R, et al. Clonal expansion of mutated mitochondrial DNA is associated with tumor formation and complex I deficiency in the benign renal oncocytoma. Hum Mol Genet. 2008; 17:986–995. [PubMed: 18156159]

Gerlinger M, Rowan A, Horswell S, Larkin J, Endesfelder D, Gronroos E, Martinez P, Matthews N, Stewart A, Tarpey P, et al. Intratumor heterogeneity and branched evolution revealed by multiregion sequencing. N Engl J Med. 2012; 366:883–892. [PubMed: 22397650]

Heidenreich B, Rachakonda P, Hemminki K, Kumar R. TERT promoter mutations in cancer development. Curr Opin Genet Dev. 2013; 24C:30–37. [PubMed: 24657534]

Ho C, Chen S, Ho K, Chan W, Leung Y, Cheng K, Wong K, Cheung M, Wong K. Dual-tracer PET/CT in renal angiomyolipoma and subtypes of renal cell carcinoma. Clin Nucl Med. 2012; 37:1075–1082. [PubMed: 22996247]

Huang FW, Hodis E, Xu MJ, Kryukov GV, Chin L, Garraway LA. Highly recurrent TERT promoter mutations in human melanoma. Science. 2013; 339:957–959. [PubMed: 23348506]

Jemal A, Simard E, Dorell C, Noone A, Markowitz L, Kohler B, Eheman C, Saraiya M, Bandi P, Saslow D, et al. Annual Report to the Nation on the Status of Cancer, 1975-2009, featuring the burden and trends in human papillomavirus(HPV)-associated cancers and HPV vaccination coverage levels. J Natl Cancer Inst. 2013; 105:175–201. [PubMed: 23297039]

Kano M, Seki N, Kikkawa N, Fujimura L, Hoshino I, Akutsu Y, Chiyomaru T, Enokida H, Nakagawa M, Matsubara H. miR-145, miR-133a and miR-133b: Tumor-suppressive miRNAs target FSCN1 in esophageal squamous cell carcinoma. Int J Cancer. 2010; 127:2804–2814. [PubMed: 21351259]

Larman TC, DePalma SR, Hadjipanayis AG, Cancer_Genome_Atlas_Research_Network. Protopopov A, Zhang J, Gabriel SB, Chin L, Seidman CE, Kucherlapati R, et al. Spectrum of somatic mitochondrial mutations in five cancers. Proc Natl Acad Sci U S A. 2012; 109:14087–14091. [PubMed: 22891333]

Lawrence M, Stojanov P, Mermel C, Robinson J, Garraway L, Golub T, Meyerson M, Gabriel S, Lander E, Getz G. Discovery and saturation analysis of cancer genes across 21 tumour types. Nature. 2014; 505:495–501. [PubMed: 24390350]

Linehan W. Genetic basis of kidney cancer: role of genomics for the development of disease-based therapeutics. Genome Res. 2012; 22:2089–2100. [PubMed: 23038766]

Mayr JA, Meierhofer D, Zimmermann F, Feichtinger R, Kogler C, Ratschek M, Schmeller N, Sperl W, Kofler B. Loss of complex I due to mitochondrial DNA mutations in renal oncocytoma. Clin Cancer Res. 2008; 14:2270–2275. [PubMed: 18413815]

Mermel CH, Schumacher SE, Hill B, Meyerson ML, Beroukhim R, Getz G. GISTIC2.0 facilitates sensitive and confident localization of the targets of focal somatic copy-number alteration in human cancers. Genome biology. 2011; 12:R41. [PubMed: 21527027]

Nickerson M, Warren M, Toro J, Matrosova V, Glenn G, Turner M, Duray P, Merino M, Choyke P, Pavlovich C, et al. Mutations in a novel gene lead to kidney tumors, lung wall defects, and benign tumors of the hair follicle in patients with the Birt-Hogg-Dube syndrome. Cancer Cell. 2002; 2:157–164. [PubMed: 12204536]

Nik-Zainal S, Alexandrov LB, Wedge DC, Van Loo P, Greenman CD, Raine K, Jones D, Hinton J, Marshall J, Stebbings LA, et al. Mutational processes molding the genomes of 21 breast cancers. Cell. 2012; 149:979–993. [PubMed: 22608084]

Pavlovich C, Walther M, Eyler R, Hewitt S, Zbar B, Linehan W, Merino M. Renal tumors in the Birt-Hogg-Dubé syndrome. Am J Surg Pathol. 2002; 26:1542–1552. [PubMed: 12459621]

Perou C, Sørlie T, Eisen M, van de Rijn M, Jeffrey S, Rees C, Pollack J, Ross D, Johnsen H, Akslen L, et al. Molecular portraits of human breast tumours. Nature. 2000; 406:747–752. [PubMed: 10963602]

Prasad SR, Narra VR, Shah R, Humphrey PA, Jagirdar J, Catena JR, Dalrymple NC, Siegel CL. Segmental disorders of the nephron: histopathological and imaging perspective. The British journal of radiology. 2007; 80:593–602. [PubMed: 17621606]

Przybycin CG, Cronin AM, Darvishian F, Gopalan A, Al-Ahmadie HA, Fine SW, Chen YB, Bernstein M, Russo P, Reuter VE, et al. Chromophobe renal cell carcinoma: a clinicopathologic study of 203 tumors in 200 patients with primary resection at a single institution. Am J Surg Pathol. 2011; 35:962–970. [PubMed: 21602658]

Rafnar T, Sulem P, Stacey S, Geller F, Gudmundsson J, Sigurdsson A, Jakobsdottir M, Helgadottir H, Thorlacius S, Aben K, et al. Sequence variants at the TERT-CLPTM1L locus associate with many cancer types. Nature genetics. 2009; 41:221–227. [PubMed: 19151717]

Reid J, Carroll A, Veeraraghavan N, Dahdouli M, Sundquist A, English A, Bainbridge M, White S, Salerno W, Buhay C, et al. Launching genomics into the cloud: deployment of Mercury, a next generation sequence analysis pipeline. BMC Bioinformatics. 2014; 15:30. [PubMed: 24475911]

Roberts SA, Lawrence MS, Klimczak LJ, Grimm SA, Fargo D, Stojanov P, Kiezun A, Kryukov GV, Carter SL, Saksena G, et al. An APOBEC cytidine deaminase mutagenesis pattern is widespread in human cancers. Nature genetics. 2013; 45:970–976. [PubMed: 23852170]

Schmidt LS, Warren MB, Nickerson ML, Weirich G, Matrosova V, Toro JR, Turner ML, Duray P, Merino M, Hewitt S, et al. Birt-Hogg-Dube syndrome, a genodermatosis associated with spontaneous pneumothorax and kidney neoplasia, maps to chromosome 17p11.2. Am J Hum Genet. 2001; 69:876–882. [PubMed: 11533913]

Shen H, Laird PW. Interplay between the cancer genome and epigenome. Cell. 2013; 153:38–55. [PubMed: 23540689]

Shuch B, Ricketts CJ, Vocke CD, Komiya T, Middelton LA, Kauffman EC, Merino MJ, Metwalli AR, Dennis P, Linehan WM. Germline PTEN Mutation Cowden Syndrome: An Under-Appreciated Form of Hereditary Kidney Cancer. The Journal of urology. 2013

Simonnet H, Demont J, Pfeiffer K, Guenaneche L, Bouvier R, Brandt U, Schagger H, Godinot C. Mitochondrial complex I is deficient in renal oncocytomas. Carcinogenesis. 2003; 24:1461–1466. [PubMed: 12844484]

Speicher MR, Schoell B, du Manoir S, Schrock E, Ried T, Cremer T, Storkel S, Kovacs A, Kovacs G. Specific loss of chromosomes 1, 2, 6, 10, 13, 17, and 21 in chromophobe renal cell carcinomas revealed by comparative genomic hybridization. Am J Pathol. 1994; 145:356–364. [PubMed: 7519827]

Storkel S, Eble JN, Adlakha K, Amin M, Blute ML, Bostwick DG, Darson M, Delahunt B, Iczkowski K. Classification of renal cell carcinoma: Workgroup No. 1. Union Internationale Contre le Cancer (UICC) and the American Joint Committee on Cancer (AJCC). Cancer. 1997; 80:987–989. [PubMed: 9307203]

The_Cancer_Genome_Atlas_Network. Comprehensive molecular portraits of human breast tumours. Nature. 2012; 490:61–70. [PubMed: 23000897]

The_Cancer_Genome_Atlas_Research_Network. Comprehensive molecular characterization of clear cell renal cell carcinoma. Nature. 2013; 499:43–49. [PubMed: 23792563]

Tickoo SK, Lee MW, Eble JN, Amin M, Christopherson T, Zarbo RJ, Amin MB. Ultrastructural observations on mitochondria and microvesicles in renal oncocytoma, chromophobe renal cell carcinoma, and eosinophilic variant of conventional (clear cell) renal cell carcinoma. Am J Surg Pathol. 2000; 24:1247–1256. [PubMed: 10976699]

Varela I, Tarpey P, Raine K, Huang D, Ong C, Stephens P, Davies H, Jones D, Lin M, Teague J, et al. Exome sequencing identifies frequent mutation of the SWI/SNF complex gene PBRM1 in renal carcinoma. Nature. 2011; 469:539–542. [PubMed: 21248752]

Ward P, Thompson C. Metabolic reprogramming: a cancer hallmark even warburg did not anticipate. Cancer Cell. 2012; 21:297–308. [PubMed: 22439925]

Weir B, Woo M, Getz G, Perner S, Ding L, Beroukhim R, Lin W, Province M, Kraja A, Johnson L, et al. Characterizing the cancer genome in lung adenocarcinoma. Nature. 2007; 450:893–898. [PubMed: 17982442]

Y C, Adams A, Robbins A, Lin Q, Khavari P. Use of human tissue to assess the oncogenic activity of melanoma-associated mutations. Nat Genet. 2005; 37:745–749. [PubMed: 15951821]

Yang L, Luquette L, Gehlenborg N, Xi R, Haseley P, Hsieh C, Zhang C, Ren X, Protopopov A, Chin L, et al. Diverse mechanisms of somatic structural variations in human cancer genomes. Cell. 2013; 153:919–929. [PubMed: 23663786]

Zhao Y, Wang S, Popova E, Grigoryev S, Zhu J. Rearrangement of upstream sequences of the hTERT gene during cellular immortalization. Genes Chromosomes Cancer. 2009; 48:963–974. [PubMed: 19672873]

Article Highlights: CANCER-CELL-D-14-00457

- Comprehensive molecular analysis of 66 kidney chromophobe cases
- Global molecular patterns provide clues as to this cancer's cell of origin
- mtDNA sequencing reveals loss-of-function mutations in NADH dehydrogenase subunits
- Genomic structural rearrangements involving TERT promoter region

Significance

Rare diseases can provide insights into the biology of more common pathologies. Using diverse molecular platforms, we deconstructed ChRCC, a tumor characterized by slow but persistent growth and high resistance to conventional cancer therapies. Global molecular patterns provide clues as to this cancer's cell of origin. MtDNA alterations represent an integral component of the molecular portrait of ChRCC. The observed TERT promoter rearrangements may result from genomic instability in precancerous cells undergoing the crisis stage of immortalization, leading to activated telomerase. These data will facilitate further discovery of driver alterations extending beyond the exome as well as the generation of hypotheses that can advance our molecular understanding of this and other cancers.

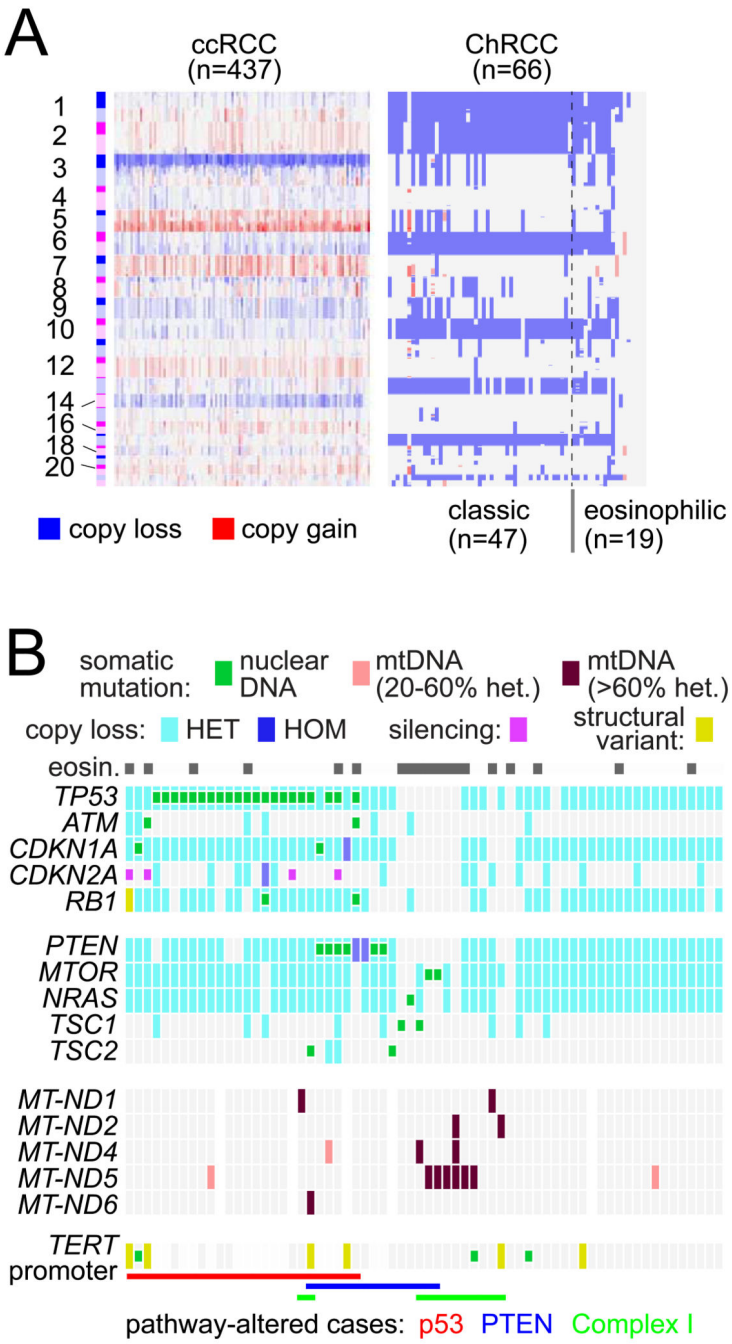

Figure 1. Gene mutations and copy alterations in Chromophobe Renal Cell Carcinoma (ChRCC)

(A) Copy number alterations (red, gain; blue, loss of one copy) by cytoband region (marker: darker color, p arm; lighter color, q arm) in ChRCC and ccRCC. **(B)** Genomic alterations in ChRCC samples, each column representing a sample. See also Figure S1 and Table S2.

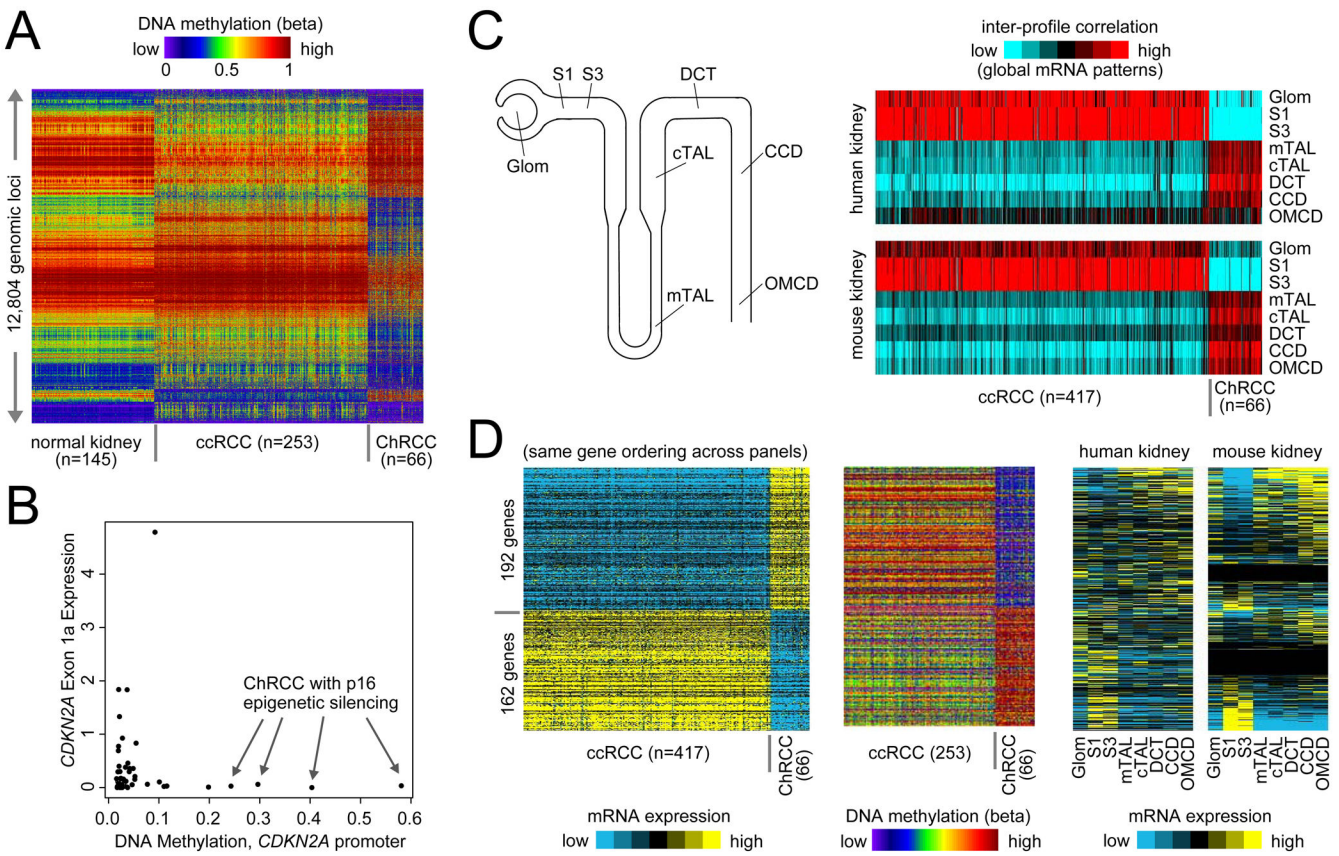

Figure 2. DNA methylation and gene expression differences between ChRCC and ccRCC

(A) Heatmap showing a randomly selected 20% of a total of 64,021 DNA methylation loci in normal kidney, ChRCC, and ccRCC (red, high; blue, low). **(B)** Epigenetic silencing of *CDKN2A* locus in four ChRCC cases. Exon 1a expression corresponds to p16INK4a isoform. **(C)** A cartoon of nephron (left) and heatmaps showing inter-sample correlations (red, positive) between profiles of kidney tumors (columns; TCGA data, arranged by subtype) and profiles of kidney nephon sites (rows; data set from Cheval *et al.*, 2012). Glom, Kidney Glomerulus; S1/S2, Kidney Proximal Tubule; MTAL, Kidney Medullary Thick Ascending Limb of Henle's Loop; CTAL, Kidney cortical Thick Ascending Limb of Henle's Loop; DCT, Kidney Distal Convoluted Tubule; CNT, Kidney Connecting Tubule; CCD, Kidney Cortical Collecting Duct; OMCD, Kidney Outer Medullary Collecting Duct. **(D)** Genes showing coordinate methylation and expression changes between ChRCC and ccRCC, with the corresponding patterns in the nephron by anatomical site. See also Figure S2 and Tables S3-S5.

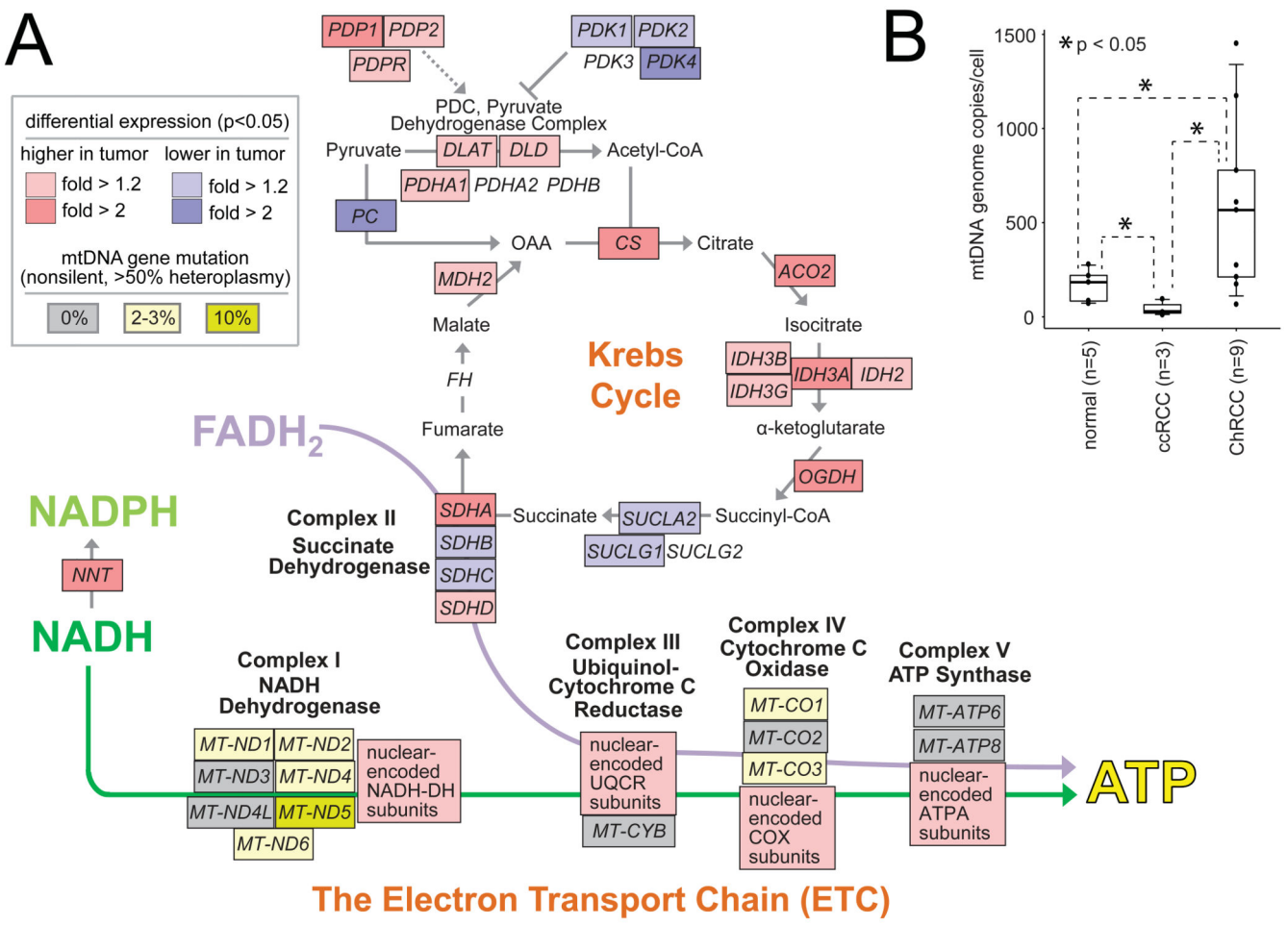

Figure 3. Molecular alterations in ChRCC involve mitochondria

(A) Mutations and gene expression differences between ChRCC and normal kidney in the context of the mitochondrion. Red and blue shading represents increased and decreased expression of nuclear-encoded genes, respectively, in ChRCC; two-sided t-test and fold change by unpaired analysis. Mutation rates are also indicated for mitochondrial DNA (mtDNA) encoded genes (not evaluated for expression): gray, no mutation; yellow, mutations detected. **(B)** mtDNA copy number analysis. p value by two-sided t-test with unequal variance. Box plots represent 5%, 25%, median, 75%, and 95%. See also Figure S3.

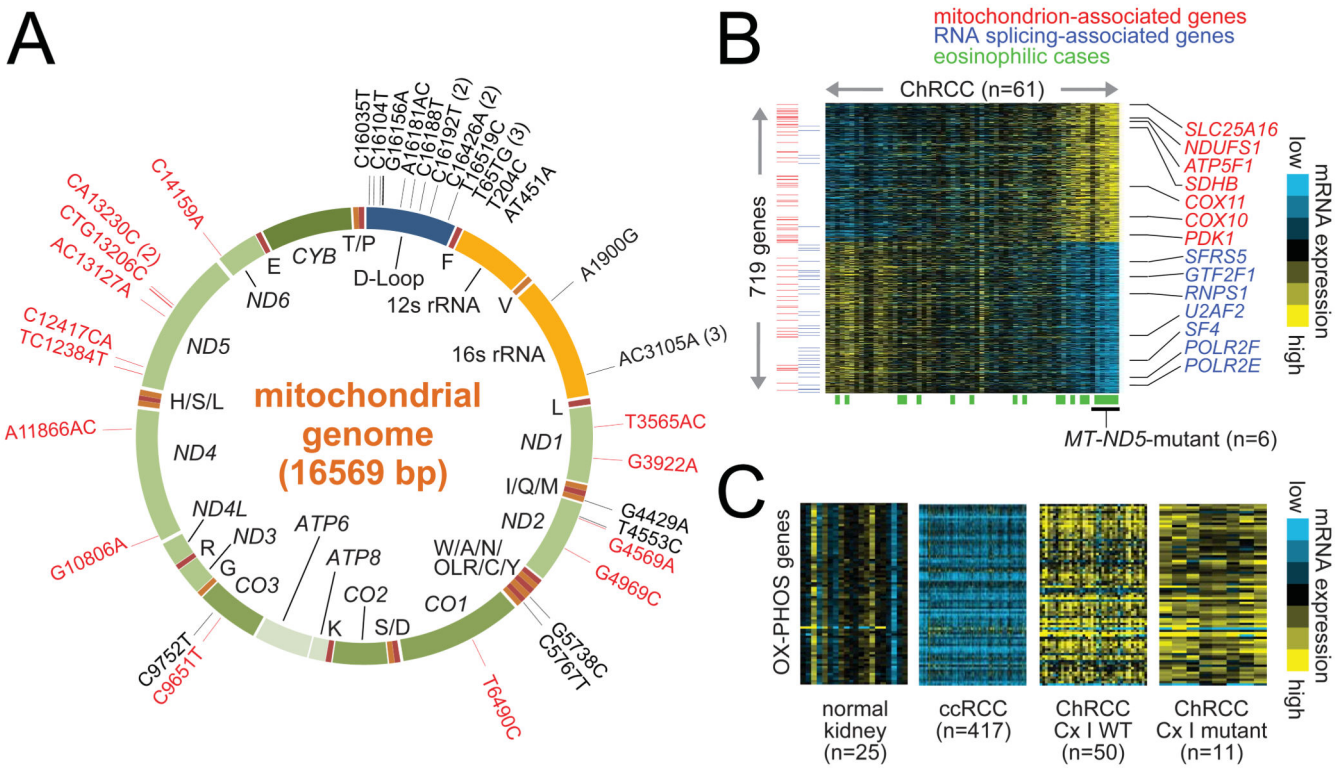

Figure 4. Integrative analysis of mtDNA mutations in ChRCC

(A) mtDNA somatic mutations (with >50% heteroplasmy) in 61 ChRCC, by LR-PCR method. Red, variants that result in amino acid change. **(B)** Gene expression difference (719 genes with p<0.001 by t-test, FDR<0.05) between ChRCC cases harboring *MT-ND5* mutations in most mtDNA copies (>70% heteroplasmy) versus other ChRCC. **(C)** Expression of nuclear-encoded subunits of Complexes I-V, or "OX-PHOS," in ChRCC and ccRCC, with (>50% heteroplasmy) or without harboring complex I (Cx I) mutations, relative to normal kidney. See also Figure S4 and Table S6.

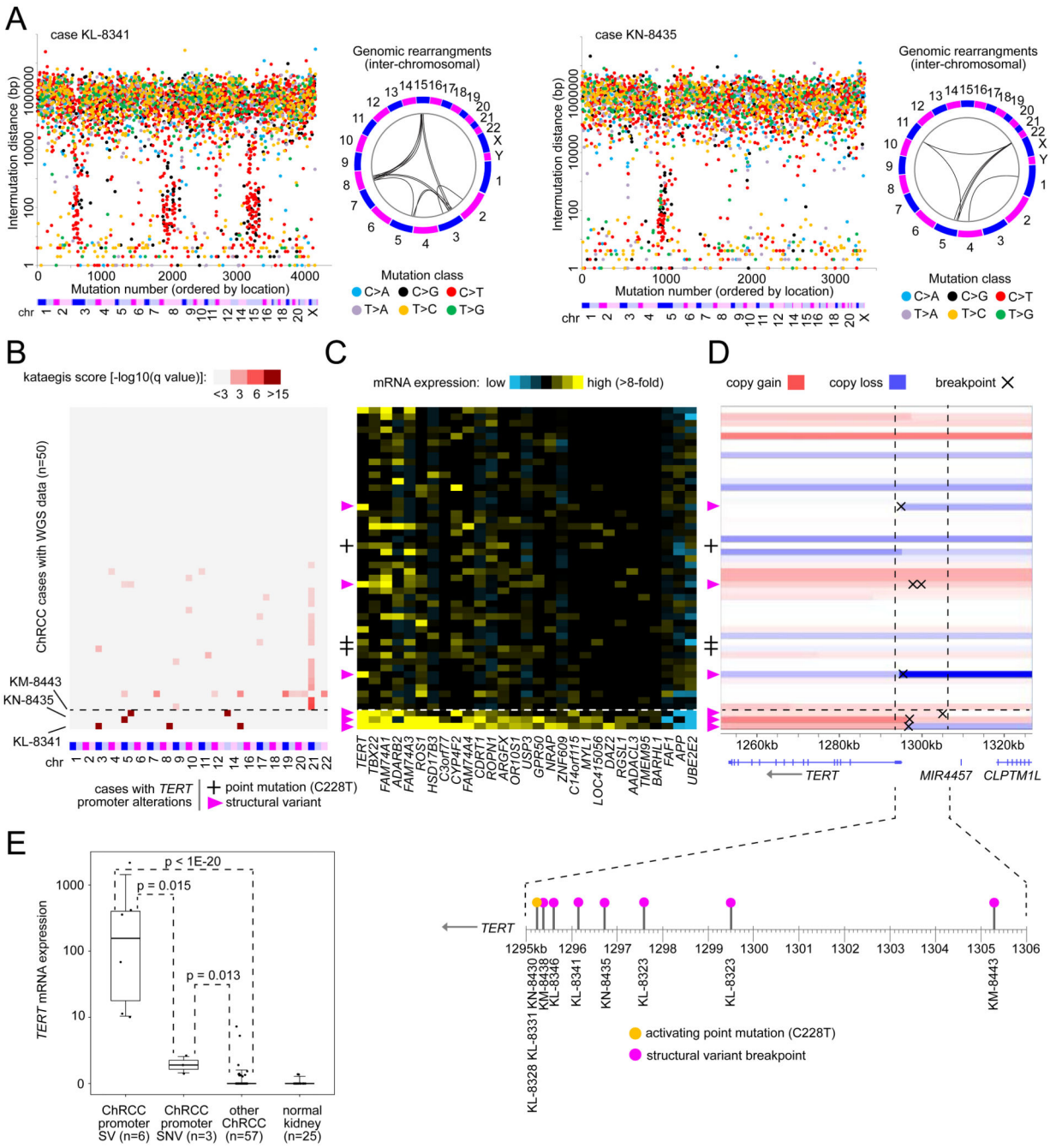

Figure 5. Kataegis and *TERT* in ChRCC

(A) Examples of a strong kataegis pattern in two ChRCC cases. 'Rainfall' plots of mutations by Whole Genome Sequencing (WGS) order events by genomic location. Vertical axis denotes genomic distance of each mutation from the previous mutation. **(B)** WGS profiles for 50 ChRCC cases, each scored by genomic region (chromosome pter/qter) for kataegis. The three ChRCC cases scoring particularly strong are indicated at the bottom. Score for a given region represents a one-sided Fisher's exact test, for enrichment of C>T or C>G mutations involving inter-mutation distances below 10 kb (corrected for testing of multiple

regions). **(C)** A set of 29 differentially expressed genes (False Discovery Rate, or FDR<0.05), including *TERT*, observed in ChRCC cases with strong kataegis versus other ChRCC. **(D)** Copy variation and DNA breakpoint analysis identifying genomic rearrangements involving the promoter region of *TERT* for the 50 ChRCC cases (case ordering the same for panels B, C, and D). The six cases harboring rearrangements involving *TERT* are indicated (pink triangles). **(E)** *TERT* expression levels in the ChRCC cases with TERT promoter Structural Variant (SV), in the ChRCC cases with *TERT* promoter mutation (SNV), and in the remaining cases, as well as in normal kidney samples. p values by two-sided t-test on log-transformed data. Box plots represent 5%, 25%, median, 75%, and 95%. See also Figure S5 and Table S7.

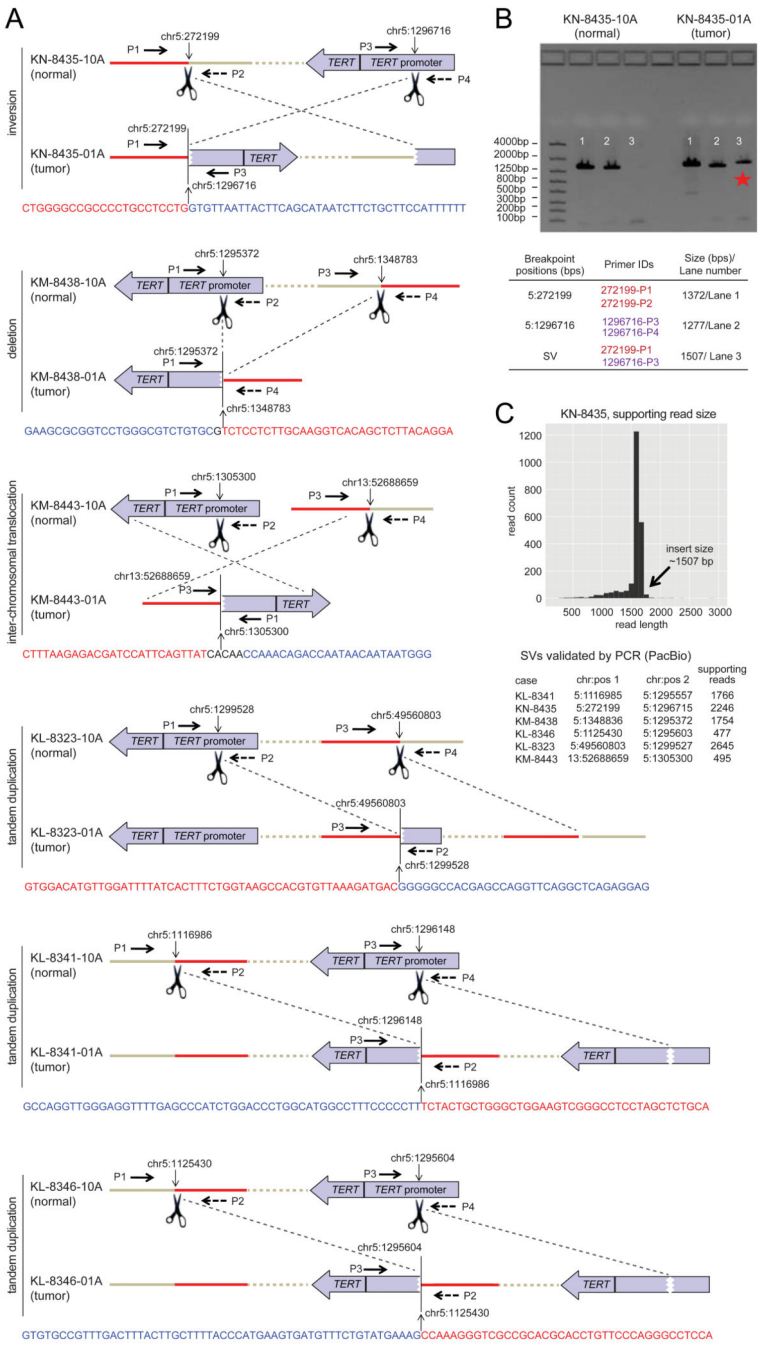

Figure 6. Genomic structural variants (SVs) involving *TERT* promoter

(A) Schematic represenation of the PCR approach used to validate *TERT* promoter SVs in the six ChRCC cases and the DNA sequence sorrounding the breaking point in each case. For each SV, PCR primers (P1/P2/P3/P4) were designed to span both sides of the breakpoint junction, as illustrated. **(B)** For case KN-8435 (as an example), DNA spanning the SV breakpoint region could be amplified in the tumor sample (but not in the paired normal sample). **(C)** For each of the six cases, amplified DNA representing SV was confirmed by sequencing (PacBio platform, which features long reads), with sufficient reads and expected

length of the PCR product being observed (top, for KN-8435), and with estimated breakpoint positions being close to those of WGS results (bottom). See also Figure S6 and Table S8.

Table 1

Summary of data types.

Data Type	Platforms	Cases	Data access
TCGA core sample set (n=66 total cases)			
Whole exome DNA sequence	Illumina	66	Controlled
Whole genome DNA sequence	Illumina	50	Controlled
Mitochondrial DNA sequence	Illumina (LR-PCR)	61	Controlled
DNA copy number/genotype	Affymetrix SNP 6	66	Controlled - CEL files Open - copy number
mRNA expression	Illumina	66	Controlled - BAM files Open - expression
miRNA expression	Illumina	66	Controlled - BAM files Open - expression
CpG DNA methylation	Illumina 450K array	66	Open

LR-PCR, Long-range polymerase chain reaction to amplify mitochondrial DNA; SNP, single nucleotide polymorphism.

See also Table S1.

Table 2

Structural variants associated with *TERT* promoter region by WGS analysis.

	breakpoint A			breakpoint B					
case	**chr:pos**	**ori***	**gene (intron)**	**chr:pos**	**ori**	**gene**	**event type**	**TERT expression****	**confirmed*****
KL-8341	5:1116986	-1		5:1296148	1	TERT PM	tandem duplication	2169.87	Yes
KN-8435	5:272199	1	*PDCD6* (I1)	5:1296716	1	TERT PM	inversion	417.42	yes
KM-8438	5:1348783	-1		5:1295372	1	TERT PM	deletion	356.10	yes
KL-8346	5:1125430	-1		5:1295604	1	TERT PM	tandem duplication	67.50	yes
KL-8323	5:49560803	1		5:1299528	-1	TERT PM	tandem duplication	10.37	yes
KL-8323	5:49563017	-1		5:1297603	1	TERT PM	deletion-insertion	10.37	no
KM-8443	13:52688659	1	*NEK5* (I4)	5:1305300	1	TERT PM	Inter-chromosomal translocation	9.13	yes

* Denotes whether the upstream (+1) or downstream (-1) sequence was fused relative to the given coordinates

** Across 66 ChRCC cases, 90th-percentile of expression for *TERT* mRNA was 5.28 units by RNA-seq.

*** Confirmation using PCR across breakpoint junction, with subsequent sequencing of PCR product by PacBio platform. No PCR product was successfully obtained for one of the two breakpoints for KL-8323, likely due in part to the complexity of rearrangements in this case.

See also Figure S7.